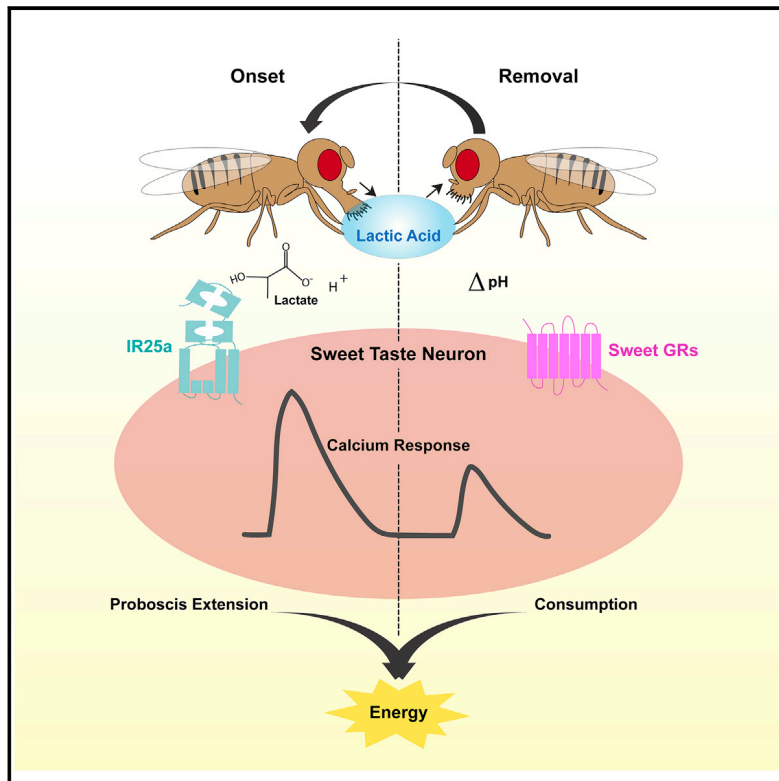


# Current Biology

## Mechanisms of lactic acid gustatory attraction in *Drosophila*

### Graphical abstract



### Authors

Molly Stanley, Britya Ghosh,  
Zachary F. Weiss, Jaime Christiaanse,  
Michael D. Gordon

### Correspondence

gordon@zoology.ubc.ca

### In brief

Stanley et al. describe the coding of attractive “sour” taste in flies. Lactic acid is strongly appetitive via activation of sweet taste neurons, which respond to both the onset and removal of acid. Each temporal phase of this response is driven by different qualities of lactic acid and mediated by different families of receptors.

### Highlights

- Lactic acid is appetitive, and its consumption provides energy to flies
- Behavioral attraction to lactic acid requires sweet taste neurons
- Sweet-taste neurons are activated by both the onset and removal of acidic stimuli
- Two different classes of receptors in sweet taste neurons detect lactate and pH



## Article

# Mechanisms of lactic acid gustatory attraction in *Drosophila*

Molly Stanley,<sup>1</sup> Britya Ghosh,<sup>1,2</sup> Zachary F. Weiss,<sup>1</sup> Jaime Christiaanse,<sup>1</sup> and Michael D. Gordon<sup>1,3,4,\*</sup><sup>1</sup>Department of Zoology and Life Sciences Institute, The University of British Columbia, 2350 Health Sciences Mall, Vancouver, BC V6T 1Z3, Canada<sup>2</sup>Graduate Program in Cell and Developmental Biology, The University of British Columbia, 2350 Health Sciences Mall, Vancouver, BC V6T 1Z3, Canada<sup>3</sup>Twitter: @Gordonflylab<sup>4</sup>Lead contact\*Correspondence: [gordon@zoology.ubc.ca](mailto:gordon@zoology.ubc.ca)<https://doi.org/10.1016/j.cub.2021.06.005>

## SUMMARY

Sour has been studied almost exclusively as an aversive taste modality. Yet recent work in *Drosophila* demonstrates that specific carboxylic acids are attractive at ecologically relevant concentrations. Here, we demonstrate that lactic acid is an appetitive and energetic tastant, which stimulates feeding through activation of sweet gustatory receptor neurons (GRNs). This activation displays distinct, mechanistically separable stimulus onset and removal phases. Ionotropic receptor 25a (IR25a) primarily mediates the onset response, which shows specificity for the lactate anion and drives feeding initiation through proboscis extension. Conversely, sweet gustatory receptors (Gr64a-f) mediate a non-specific removal response to low pH that primarily impacts ingestion. While mutations in either receptor family have marginal impacts on feeding, lactic acid attraction is completely abolished in combined mutants. Thus, specific components of lactic acid are detected through two classes of receptors to activate a single set of sensory neurons in physiologically distinct ways, ultimately leading to robust behavioral attraction.

## INTRODUCTION

Tastants are canonically classified as belonging to a single taste modality, which is generally sensed by one receptor or family of receptors. However, gustatory detection of some chemical species can be complex, with specific molecular properties differentially acting on multiple receptors. For example, artificial sweeteners can activate both sweet and bitter receptors, NaCl is detected as Na<sup>+</sup> and Cl<sup>-</sup> through multiple receptors in different types of gustatory cells, and many bitter compounds inhibit insect sweet receptors.<sup>1–8</sup> Although acids are a particularly diverse class of ligands containing a large variety of side chains in addition to being protonated, how the properties of individual acids influence gustatory detection remains unclear.

Acid sensing by the gustatory system, or “sour taste,” is traditionally thought to prevent animals from ingesting potentially harmful spoiled or unripe foods.<sup>9–14</sup> Thus, sour has been studied almost exclusively as an aversive taste modality in both mammals and invertebrates.<sup>9,10,15,16</sup> The proton channel Otop1 mediates low pH detection by mammalian taste receptor cells.<sup>9,17,18</sup> However, it has been known for a century that “sourness” varies among acids, even at the same pH, suggesting that acid taste involves more than the detection of protons.<sup>19,20</sup> This may be particularly relevant for weak acids that are regularly consumed in nutritious foods,<sup>21,22</sup> including those having undergone fermentation or preservation.

Recent studies in the fruit fly, *Drosophila melanogaster*, demonstrate that, while all acids are aversive at high concentrations and

low pH, some are attractive at lower concentrations.<sup>15</sup> For example, acetic acid and lactic acid can both encourage feeding, likely signaling the presence of energy or beneficial microbes.<sup>23</sup> Appetitive responses to acetic acid are starvation dependent and require sweet gustatory receptor neurons (GRNs).<sup>24</sup> The specific receptors involved in acid feeding are unclear, but two broadly expressed ionotropic receptors (IRs), IR25a and IR76b, mediate acid detection during egg laying.<sup>25</sup> A more specific IR subunit, IR7a, mediates rejection of concentrated acetic acid but has no role in attraction.<sup>15</sup> These studies in flies highlight the roles of the specific anion, concentration, and pH in sour taste and feeding behavior.

To probe the molecular mechanisms of acid detection, we focused on lactic acid attraction. Lactic acid is particularly appetitive to flies<sup>15</sup> and increases lifespan, suggesting that its consumption is beneficial.<sup>26</sup> We show that lactic acid feeding attraction requires sweet taste neurons, but not olfaction. Interestingly, lactic acid produces unusual response dynamics in sweet GRNs, which show calcium peaks during both stimulus onset and removal. The two peaks are mediated by distinct receptor families, with onset requiring IR25a and removal responses requiring members of the sweet gustatory receptor (GR) family. Mutation of either family leaves lactic acid attraction largely intact, suggesting that both onset and removal peaks are salient during feeding. However, flies carrying mutations in both receptor types completely lack attractive lactic acid taste. These data support a unique model for acid taste where two co-expressed receptor



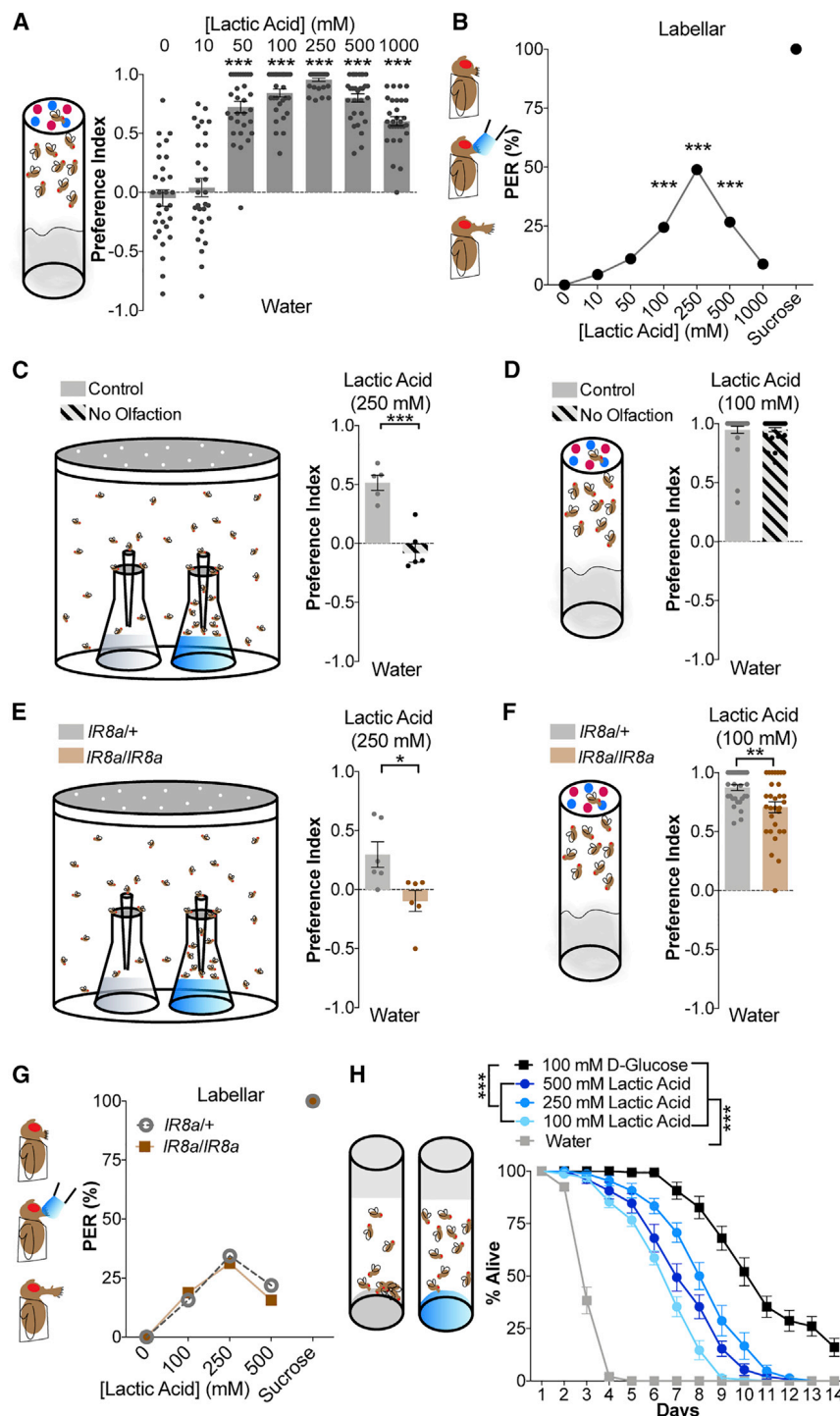


**Figure 1. Lactic acid is an appetitive taste to *Drosophila***

(A) Dye-based feeding assay schematic (left) and feeding preferences in *w<sup>1118</sup>* flies. *n* = 30 groups of 10 flies.

(B) Labellar PER schematic (left) and lactic acid PER in *w<sup>1118</sup>* flies. *n* = 45 flies, dots represent the mean. 500 mM sucrose was a control.

(C) Olfactory trap assay schematic (left) and olfactory attraction in *w<sup>1118</sup>* flies with or without antennae and maxillary palps removed. *n* = 5 groups of 40 flies.

(D) Feeding preference of *w<sup>1118</sup>* flies without olfaction. *n* = 30 groups of 10 flies.

(E and F) Preferences of *IR8a* mutants in the olfactory trap assay (E; *n* = 6 groups of 40 flies) and binary feeding assay (F; *n* = 30 groups of 10 flies).

(G) Labellar PER of *IR8a* mutants. *n* = 32 flies per genotype, dots represent the mean. 500 mM sucrose was a control.

(H) Survival of *w<sup>1118</sup>* flies on indicated solutions. Points represent mean  $\pm$  SEM; *n* = 15 groups of 10 flies.

All bars represent mean  $\pm$  SEM. Asterisks denote significant difference from 0 mM by one-way ANOVA with Dunnett's post-test (A and B) and differences between groups by unpaired *t* test (C–F) or two-way ANOVA with Tukey's post-test (H); \**p* < 0.05, \*\**p* < 0.01, and \*\*\**p* < 0.001. See Figure S1.

attraction at 250 mM and attraction at concentrations from 50 mM to 1 M (Figure 1A). This remained true for mated and virgin *w<sup>1118</sup>* females, *w<sup>1118</sup>* males, and *Canton S* females and males (Figure S1A). To ensure that lactic acid preference in the dye-based assay was an accurate reflection of consumption, we measured preference across the same range of concentrations using the Capillary Feeder (CAFE) assay and saw nearly identical results (Figure S1B). Importantly, this also revealed that lactic acid preference over water is a reliable indicator of total lactic acid consumption, and preference is maintained over 24 h (Figures S1C and S1D). We also quantified the proboscis extension reflex (PER) as a measure of feeding initiation. Stimulation of labellar taste sensilla with lactic acid produced dose-dependent PER that mirrored feeding, with maximum response frequency around 250 mM (Figure 1B). Tarsal PER responses were weak but significant from 100 mM to 500 mM (Figure S1E).

families mediate distinct physiological responses to a pure chemical in a single sensory neuron type.

## RESULTS

### Lactic acid is an appetitive taste to *Drosophila*

Consistent with a previous report,<sup>15</sup> flies strongly preferred lactic acid over water in a dye-based binary feeding assay, with peak

As expected, surgical removal of the olfactory organs eliminated lactic acid attraction in an olfactory trap assay (Figure 1C). However, the same surgery had no effect on preference in the binary feeding assay, indicating that olfaction is dispensable for lactic acid feeding attraction (Figure 1D). As independent verification, we saw that mutants for *IR8a*, which mediates lactic acid olfactory attraction in *Aedes aegypti*<sup>27</sup> and olfactory acid aversion in *Drosophila*,<sup>13</sup> showed no olfactory attraction to lactic

acid but maintained strong feeding preference (Figures 1E and 1F). Although this preference was slightly reduced in *IR8a* mutants compared to controls, PER responses were normal (Figures 1G and S1F). Therefore, appetitive taste and feeding responses to lactic acid are largely independent of olfaction.

To investigate a potential reason for flies' strong attraction to lactic acid, we quantified the ability of lactic acid to provide energy. We found that lactic acid presented as the sole energy source significantly promoted survival, although to a lesser extent than D-glucose (Figure 1H). Thus, lactic acid is an appetitive, attractive, and energetic compound for *Drosophila*.

### Sweet GRNs are necessary for lactic acid feeding attraction

To examine the cellular basis of attractive lactic acid taste, we used Kir2.1 to silence five distinct GRN classes encompassing almost every taste neuron on the fly labellum.<sup>5</sup> Only sweet GRNs, labeled by *Gr64f-Gal4*, were required for lactic acid attraction and PER (Figures 2A–2C). Notably, flies lacking sweet taste showed concentration-dependent avoidance of lactic acid, suggesting that lactic acid stimulates a parallel aversive pathway (Figure 2B). Because *Gr64f-Gal4* is also expressed in olfactory receptor neurons (ORNs) projecting to the antennal lobe (Figure S2A),<sup>28</sup> we repeated the olfactory trap assay with *Gr64f*-silenced flies and found no change in lactic acid attraction (Figure S2B). We also silenced a majority of sweet GRNs using *Gr64e-Gal4*, which has no olfactory expression (Figure S2C), and saw elimination of lactic acid feeding attraction (Figure S2D).

Next, we recorded GCaMP6f calcium responses in sweet GRN axon terminals (Figure 2E). As expected, standard 1-s stimulations<sup>5</sup> revealed strong responses to lactic acid (Figure 2D). However, we noted an emergence of two peaks at 500 mM: one coinciding with stimulus onset and one with removal. We repeated the imaging experiment with 4-s stimulations to allow better separation of the two peaks. This revealed a distinct removal peak to 250 mM lactic acid and above, but not in response to sucrose (Figure 2F). Interestingly, the two lactic acid peaks appeared somewhat spatially distinct in the SEZ, with removal activity enriched in dorsal *Gr64f* projections (Figure 2G). Indeed, the more ventral subset of sweet GRNs labeled by *IR56d-Gal4*<sup>29</sup> exhibits robust onset responses to 500 mM lactic acid, with little to no removal peak (Figure 2H).

### pH influences both onset and removal calcium peaks in GRNs

100 mM lactic acid has a pH of ~3, while 500 mM has a pH of ~2. Because emergence of removal responses is correlated with the lower pH of higher acid concentrations, we tested the effect of adjusting 100 mM lactic acid to a pH of 2 or 7. We found that 100 mM lactic acid at pH 2 evoked a lower onset peak and stronger removal peak compared with control lactic acid, exhibiting kinetics more closely resembling responses to higher concentrations (Figure 3A). Moreover, HCl at the same pH elicited minimal onset activity but a significant removal response (Figure 3A). Conversely, neutralized lactic acid produced no removal peak. This was not an effect of adding Na<sup>+</sup> during pH adjustment, as addition of NaCl to the control had no appreciable effect on the responses. Based on these experiments, we posited a model in which two distinct chemical properties of lactic acid act on

sweet GRNs: lactate anions evoke a strong, specific onset response, while acidity contributes to onset responses and also produces prominent removal peaks (Figure 3B).

Because other carboxylic acids are known to activate bitter GRNs,<sup>10</sup> we tested whether bitter neurons contribute to lactic acid taste. Short (1-s) lactic acid stimulations produced dose-dependent responses with kinetics similar to caffeine (Figures S3A and S3B). However, longer (4-s) stimulations revealed that lower lactic acid concentrations primarily produce calcium peaks upon stimulus removal (Figures S3C and S3D). At higher concentrations (500 mM), calcium levels increased from stimulus onset and remained elevated (Figure S3D). Our panel of pH-adjusted solutions also revealed sustained responses to pH 2 solutions, with strongest activation from pH 2 lactic acid (Figure S3E). Although 100 mM NaCl is known to minimally activate bitter GRNs,<sup>5</sup> its addition to the pH 3 lactic acid (to control for the Na<sup>+</sup> in pH 7 lactic acid) appeared to produce an onset peak not seen from pure 100 mM lactic acid. However, most interestingly, neutral lactic acid produced no response in bitter GRNs, despite the presence of Na<sup>+</sup> (Figure S3E).

The co-activation of sweet and bitter GRNs by lactic acid is consistent with our behavioral experiments revealing dose-dependent aversion in the absence of sweet GRN function (Figure 2B). Thus, stimulation of sweet GRNs overrides bitter GRN activity to drive lactic acid feeding (Figure 3C). Because we were most interested in the mechanisms of lactic acid attraction, we focused entirely on sweet GRN responses going forward.

### IR25a mediates onset responses

IR25a is a broadly expressed co-receptor required for most IR-mediated taste detection, including acid detection by tarsal “sour” GRNs during oviposition.<sup>5,30–32</sup> Mild defects in acetic acid PER have been reported for *IR25a* mutants,<sup>24</sup> and IR25a was a candidate receptor for propionic acid feeding attraction in *Drosophila* larvae.<sup>14</sup> To examine a potential role for IR-dependent taste in lactic acid attraction, we tested *IR25a* mutants and found a strong but incomplete reduction in lactic acid PER (Figure 4A). However, these mutants show only a slight reduction in preference for lactic acid in the binary feeding assay (Figure 4B). Because IR25a is broadly expressed in chemosensory neurons, we rescued IR25a specifically in sweet GRNs and found that this restored normal lactic acid feeding preference (Figure 4B). These data indicate that flies possess IR25a-dependent and IR25a-independent mechanisms for gustatory attraction to lactic acid and that IR25a appears to play a more prominent role in proboscis extension than consumption. We also examined IR76b, another broad IR co-receptor; however, *IR76b* mutants had no reduction in lactic acid PER or feeding preferences, instead showing marginally increased attraction at some concentrations (Figures 4C and 4D).

Consistent with our behavioral data, calcium imaging of *IR25a* mutants revealed partial but significant reductions in sweet GRN responses to 1-s lactic acid stimuli, which were rescued by cell-type-specific expression of *IR25a* (Figure 4E). Using 4-s stimulations to separate response phases, we observed significantly reduced onset peaks in *IR25a* mutants at all concentrations, with no effect on removal peaks (Figure 4F). Qualitatively, the reduction in onset responses appeared primarily in the ventral (IR56d+) projection area, leaving residual onset and normal



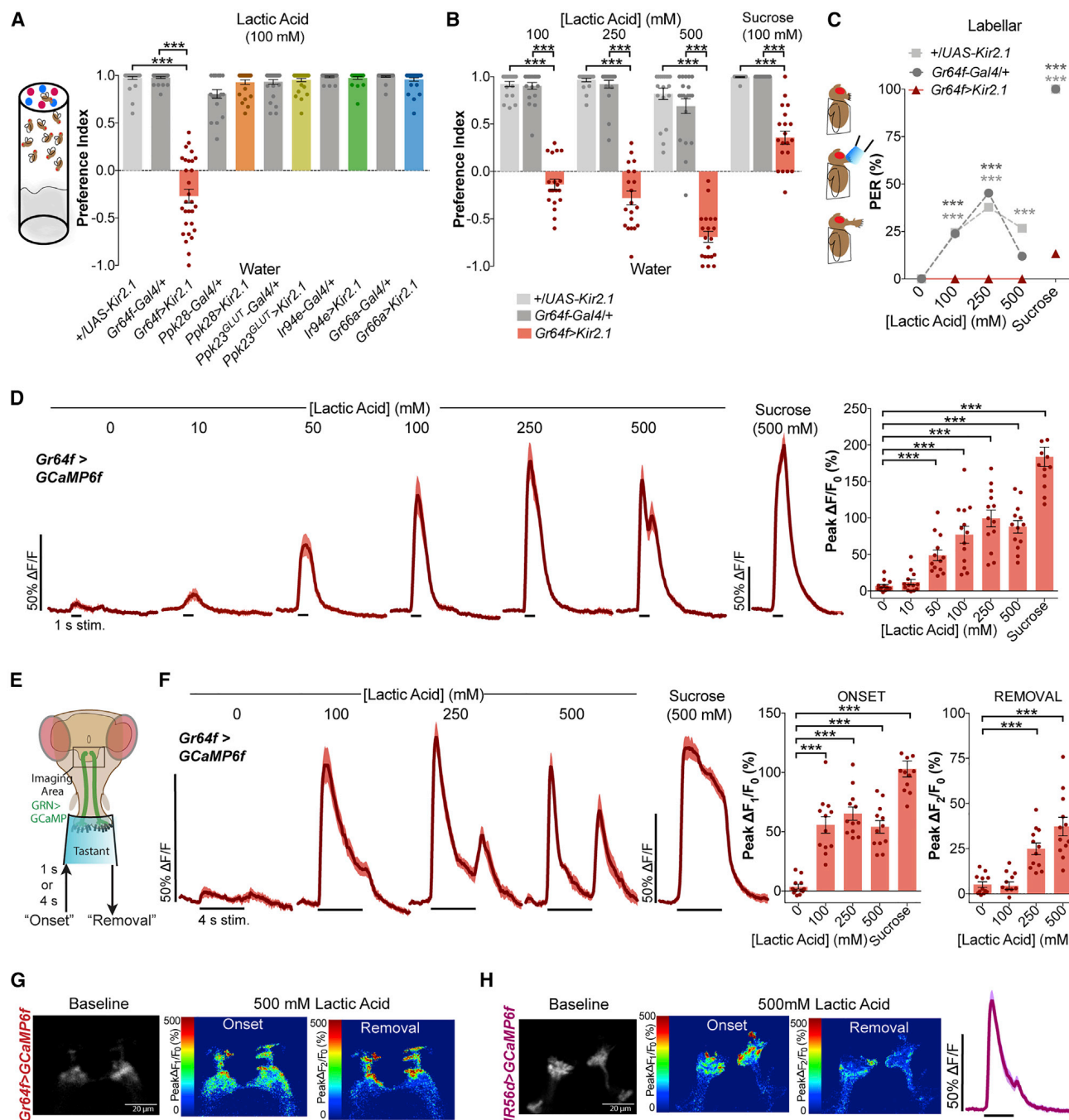


**Figure 2. Sweet GRNs are necessary for lactic acid feeding attraction**

(A) Feeding preferences with Kir2.1 silencing of distinct GRN classes. <sup>5</sup> n = 20–36 groups of 10 flies.

(B) Feeding preferences with sweet GRN silencing. n = 20 groups of 10 flies.

(C) Labellar PER with sweet GRN silencing. n = 42–45 flies; dots represent the mean. 500 mM sucrose was a control. See Figure S2.

(D) *Gr64f>GCaMP6f* sweet GRN calcium responses to 1-s stimulations, showing time course (left) and peak fluorescence changes (right). n = 13 flies.

(E) Schematic of *in vivo* calcium imaging preparation.

(F) Sweet GRN calcium responses to 4-s stimulations, with “onset” and “removal” peak fluorescence changes. n = 12 flies.

(G) Heatmap of *Gr64f>GCaMP6f* fluorescence changes with 500 mM lactic acid onset versus removal.

(H) Heatmaps (left) and time course (right) of *IR56d>GCaMP6f* fluorescence changes with 500 mM lactic acid onset versus removal. n = 15 flies.

All fluorescence time course lines and shaded areas represent mean  $\pm$  SEM. All bars represent mean  $\pm$  SEM. Asterisks denote significant differences by one-way ANOVA (A) or two-way ANOVA (B and C) with Tukey’s post-test and difference from 0 mM by one-way ANOVA with Dunnett’s post-test (D and E); \*\*\*p < 0.001. See Figure S2.

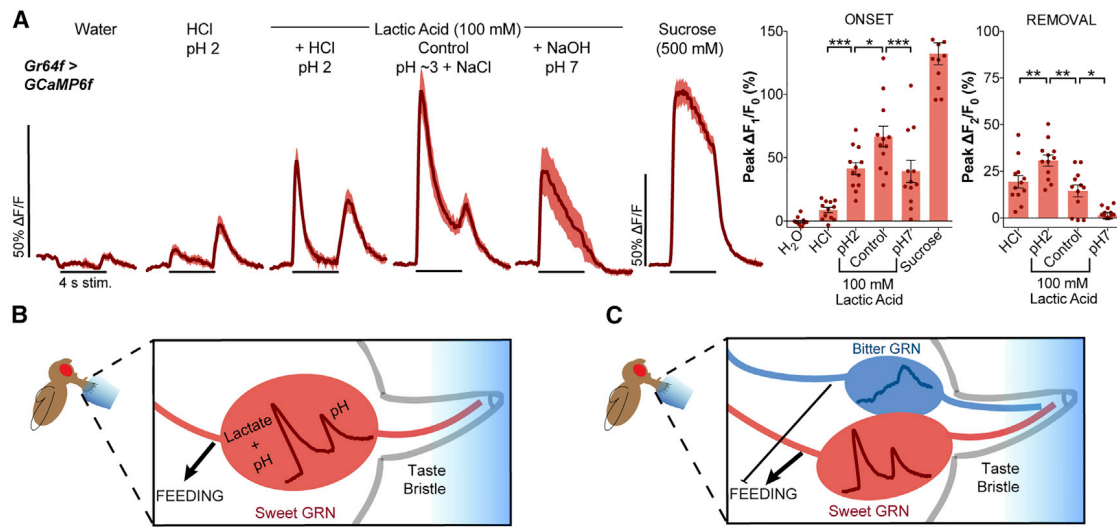


**Figure 3. pH influences both onset and removal calcium peaks in GRNs**

(A) Sweet GRN calcium responses to pH-adjusted 100 mM lactic acid and control solutions. 100 mM NaCl was added to pH ~3 lactic acid to control for the presence of Na<sup>+</sup> in neutralized stimulus. Lines and shaded areas represent mean  $\pm$  SEM over time (left); bars represent mean  $\pm$  SEM of onset and removal peak fluorescence changes (right). n = 12 flies. Asterisks denote significant differences compared to control 100 mM lactic acid by one-way ANOVA with Sidak's post-test; \*p < 0.05, \*\*p < 0.01, and \*\*\*p < 0.001.

(B) Model of a sweet GRN: onset is driven by lactate plus low pH, and the removal peak is generated by pH.

(C) Model of how lactic acid responses in sweet and bitter GRNs influence feeding behavior.

See [Figure S3](#) for bitter GRN imaging.

removal responses in the dorsal (IR56d<sup>-</sup>) region of the SEZ ([Figure S4A](#)). Notably, although NaCl responses are *IR25a*-dependent,<sup>5</sup> they do not display a removal peak, demonstrating that this is not a general property of IR25a activation ([Figures 4E and 4F](#)). Together, our results suggest a model in which IR25a mediates sweet GRN onset responses to the lactate anion, while an independent mechanism drives non-specific onset and removal responses to acidic stimuli.

### Sweet GRs mediate removal responses

A screen of candidate IR genes that could participate in lactic acid detection revealed no defects in behavioral attraction ([Figure S4B](#)). Therefore, we turned to sweet GRs, which detect sugars and represent the other major class of receptors found in sweet GRNs.<sup>33–36</sup> Surprisingly, every sweet GR mutant we tested showed a significant reduction in lactic acid attraction ([Figure 5A](#)). However, the strongest phenotype appeared in *Gr64a*<sup>2</sup> mutants, which have a deletion covering *Gr64a*, *Gr64b*, and *Gr64c*.<sup>35</sup> An independent deletion of the entire *Gr64* cluster of six sweet GRs ( $\Delta$ *Gr64a-f*) produced an equivalent phenotype, which was not enhanced by further removal of the three remaining sweet GRs ( $\Delta$ 8 sugar GRs; *Gr43a*<sup>GAL4</sup>). In order to probe the role of GRs in lactic acid taste, we continued by primarily studying the  $\Delta$ *Gr64a-f* deletion because it combined a strong phenotype with access to more feasible genetic manipulations.

$\Delta$ *Gr64a-f* mutants display strongly reduced feeding preference for lactic acid ([Figure 5B](#)). However, they do not show the clear switch to behavioral aversion evident with sweet GRN silencing, highlighting the existence of a GR-independent pathway for lactic acid attraction ([Figure 2B](#)). Strikingly, we found that  $\Delta$ *Gr64a-f* mutants have substantially elevated PER to lactic acid ([Figure 5C](#)), and single mutants for *Gr61a*, *Gr64d*, or *Gr64f*

have varying levels of PER enhancement ([Figures S5A–S5C](#)). This is consistent with a prior report showing enhanced PER to acetic acid in sweet GR mutants<sup>24</sup> and presents a paradoxical mismatch between the apparent role of sweet GRs in the binary feeding assay and PER.

In an attempt to reconcile these opposing behavioral results, we performed calcium imaging in  $\Delta$ *Gr64a-f* mutants. 1-s stimulations, which most closely mimic the stimulus timing in PER, revealed stronger responses in  $\Delta$ *Gr64a-f* mutants at concentrations from 10 to 100 mM but similar responses to 250–500 mM, likely because of a ceiling effect ([Figure 5D](#)). 4-s stimulations produced two trends: the onset peaks trended higher in the mutants, and the removal peaks were lower, with significance at a concentration of 500 mM ([Figure 5E](#)). Qualitatively, the localization of onset and removal responses in SEZ projections was also less separable in  $\Delta$ *Gr64a-f* mutants, which displayed little activity in the dorsal sweet projections ([Figure S5D](#)).

Because GR mutations reduced the pH-sensitive removal response, we next investigated the interaction of GRs and pH by performing pH-adjusted 100 mM lactic acid stimulations in  $\Delta$ *Gr64a-f* mutants. Strikingly,  $\Delta$ *Gr64a-f* mutants completely lacked the removal peak evoked by pH 2 lactic acid ([Figure 5F](#)). Moreover, the onset enhancement of  $\Delta$ *Gr64a-f* mutants was absent in response to neutral lactic acid ([Figure 5F](#)). These results point to a role for sweet GRs that is opposite to that of IR25a: GRs mediate the second peak to acid removal and have a minor effect on limiting the onset peak. The GR-mediated removal response also appears sensitive to GR dose, as heterozygous controls lacked a removal peak to HCl alone ([Figure 5F](#)). Taken together, our data suggest that sweet GRs mediate acid removal responses that play an important role in consumption but are dispensable for proboscis extension.

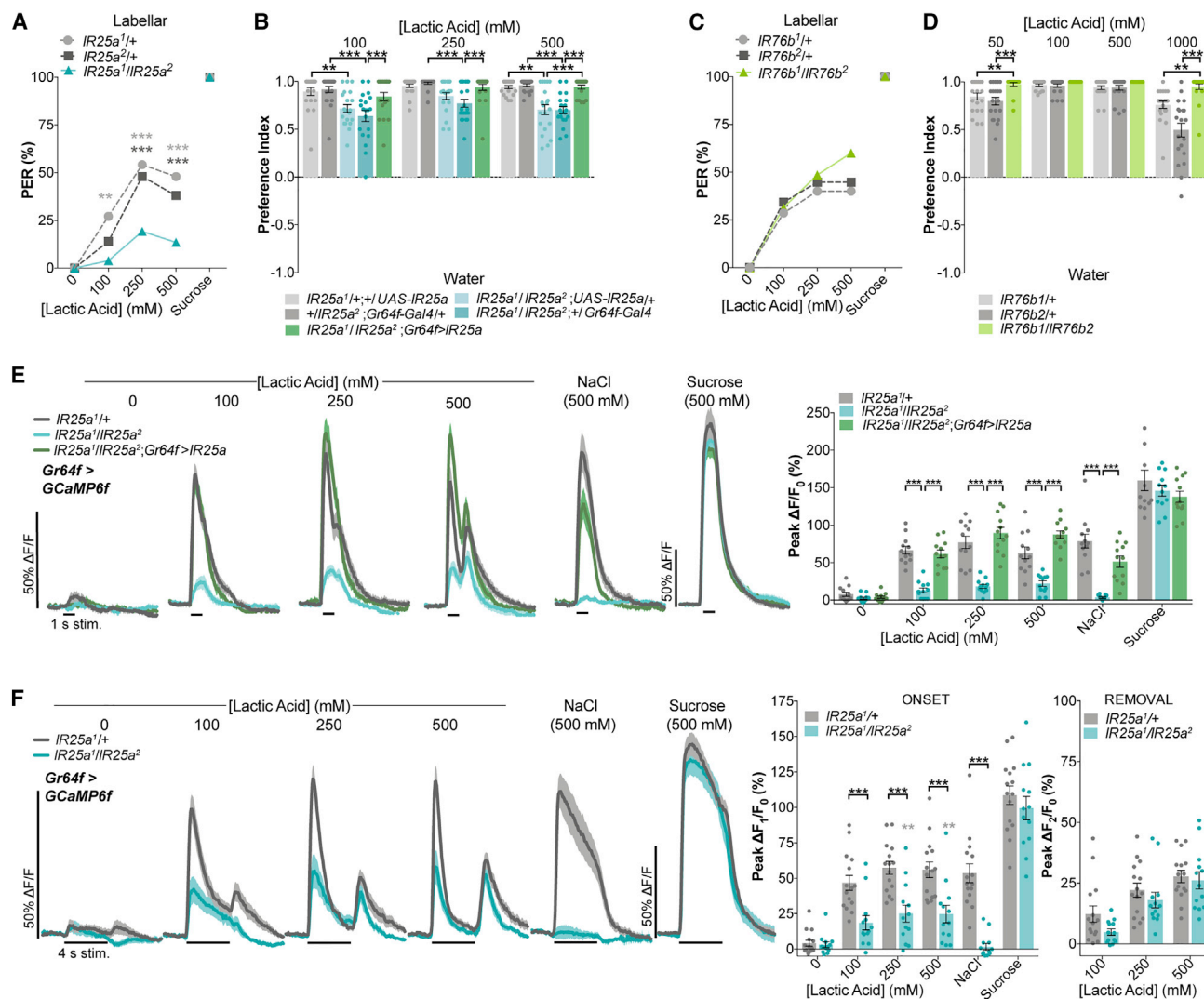


**Figure 4. IR25a mediates onset responses**

(A) Labellar PER in *IR25a* mutants. *n* = 48–52 flies per genotype.  
 (B) Feeding preferences of *IR25a* mutants and sweet GRN rescue of *IR25a*. *n* = 20 groups of 10 flies.  
 (C) Labellar PER of *IR76b* mutants. *n* = 35–38 flies per genotype.  
 (D) Feeding preferences of *IR76b* mutants. *n* = 20 groups of 10 flies per genotype per concentration.  
 (E) Sweet GRN calcium imaging in *IR25a* mutants and sweet GRN rescue of *IR25a* with 1-s stimulation. *n* = 12 flies.  
 (F) Sweet GRN calcium responses with 4-s stimulations, with onset and removal peaks quantified (right). *n* = 13–15 flies.  
 All calcium imaging lines and shaded areas represent mean ± SEM. All bars represent mean ± SEM. For PER, dots represent mean and 500 mM sucrose is used as a control. Asterisks denote significant differences by two-way ANOVA with Tukey's post-test (A–E) or Sidak's post-test (F); gray asterisks in (F) denote significance within mutants by one-way ANOVA with Dunnett's post-test compared to water; \*\**p* < 0.01 and \*\*\**p* < 0.001. See Figure S4.

**Lactic acid attraction is abolished in combined mutants for *IR25a* and sweet GRs**

Calcium imaging of flies with mutations in both *IR25a* and  $\Delta$ *Gr64a-f* revealed a complete loss of sweet GRN sensitivity to lactic acid (Figures 6A and 6B). While NaCl responses were also lost due to the *IR25a* mutation, small residual sucrose responses demonstrated that the GRNs were still intact and functional (Figures 6A and 6B). Consistent with the physiology, labellar PER to lactic acid was completely eliminated in combined mutants (Figure 6C), and lactic acid preference in the binary choice feeding assay was shifted to aversion that was equivalent or stronger than with sweet GRN silencing (Figure 6D). These experiments

confirm that appetitive lactic acid detection is mediated by two receptor families that each contribute to distinct components of the physiological response and that these responses are only abolished upon removal of both receptor types.

**Differentiation between lactic and other attractive acids requires *IR25a***

Our model for attractive lactic acid taste posits that *IR25a* primarily detects the lactate anion while sweet GRs more generally respond to low pH. One prediction of this model is that sweet GR mutants should still prefer lactic acid over less attractive carboxylic acids, but *IR25a* mutants should lose this distinction. Guided by previous





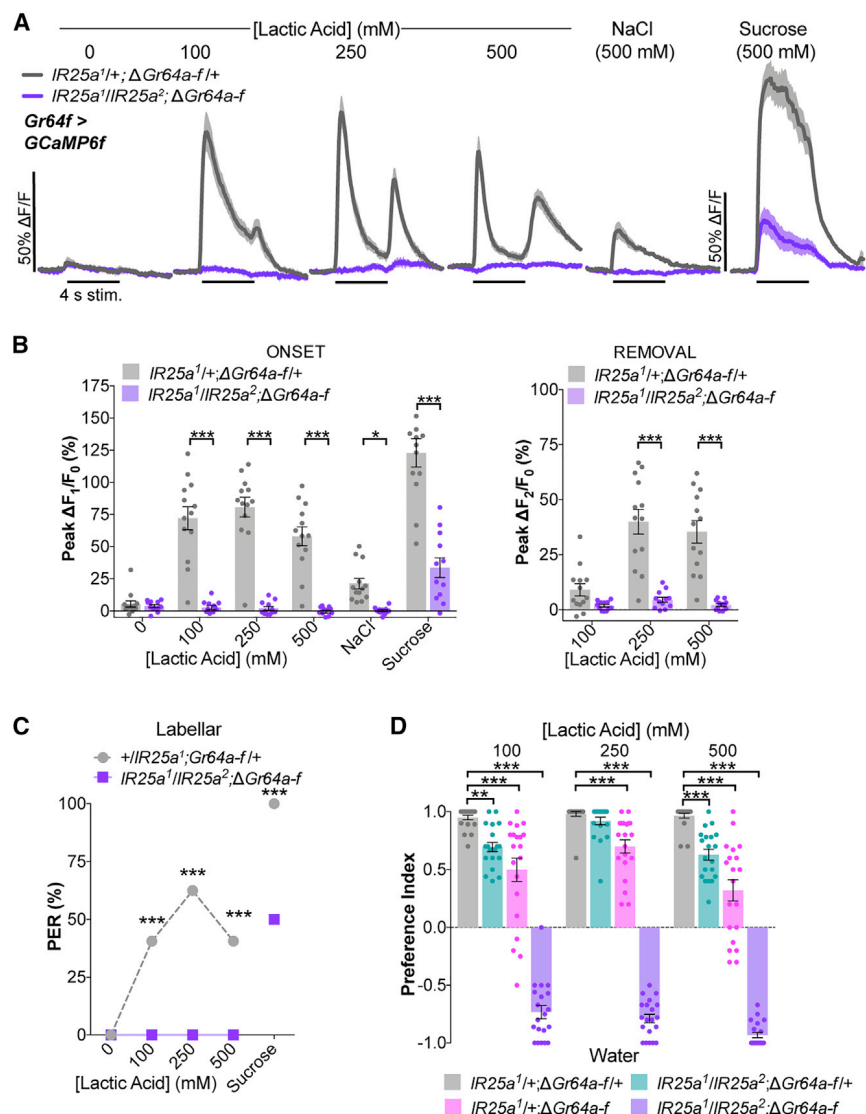


**Figure 6. Lactic acid attraction is abolished in combined mutants for IR25a and sweet GRs**

(A) Sweet GRN calcium imaging in *IR25a*,  $\Delta$ *Gr64a-f* mutants with 4-s stimulations. Lines and shaded areas represent mean  $\pm$  SEM.

(B) Quantification of onset and removal peak fluorescence changes.  $n = 12$ –13 flies.

(C) Labellar PER of *IR25a*,  $\Delta$ *Gr64a-f* mutants.  $n = 32$  flies per genotype; dots represent the mean. 500 mM sucrose was a control.

(D) Feeding preferences of *IR25a*,  $\Delta$ *Gr64a-f* mutants.  $n = 20$  groups of 10 flies.

All bars represent mean  $\pm$  SEM. Asterisks denote significant differences by two-way ANOVA with Sidak's post-test (B), Tukey's post-test (C), or Dunnett's post-test (D); \* $p < 0.05$ , \*\* $p < 0.01$ , and \*\*\* $p < 0.001$ .

attraction to lactic over propionic acid was mildly reduced in the mutants, mutants still consumed significantly more lactic acid (Figure S6D). In line with this behavior, calcium responses in  $\Delta$ *Gr64a-f* mutants remained significantly higher for lactic acid than the other acids (Figure 7F). Together, our data from individual mutants and *IR25a*,  $\Delta$ *Gr64a-f* combined mutants, which completely lose attraction to all three acids (Figure 7G), supports the conclusion that sweet GRs non-specifically respond to low pH and the IR25a-containing receptor is differentially tuned to specific acids.

Finally, to explain the relative attractiveness of different acids, we compared the ability of all three to serve as a sole energy source. We found that lactic acid had the most significant positive impact on survival, followed closely by acetic acid (Figure 7H). Propionic acid minimally prolonged survival, and HCl, as a pH control, produced the same results as water.

## DISCUSSION

The mechanisms of sour taste detection have been particularly difficult to identify because a large proportion of proteins have the potential to respond to acids either directly or indirectly.<sup>37</sup> By using *Drosophila melanogaster*, we were able to assess more nuanced aspects of acid taste *in vivo* and determine the impact of different acid components on feeding behavior. Our results reveal an unprecedented complexity in the chemoreception of lactic acid, where different classes of receptors are required for the detection of the anion and pH and both are required for aspects of feeding (Figures 7I and 7J).

### Onset and removal responses in labellar GRNs

Similar onset and removal kinetics to what we describe in sweet GRN acid responses were recently shown in bitter GRN responses

reports,<sup>14,15,24</sup> we began by confirming that 100 mM concentrations of acetic and propionic acids are appetitive and activate sweet GRNs but to a lesser extent than lactic acid (Figures S6A and S6B). As expected, *IR25a* mutants show only minor reductions in attraction to all three acids (Figure 7A). To accurately measure relative attraction, we used a volumetric CAFE assay to measure preference between 200 mM concentrations of lactic acid and each of the other two acids, all with a pH of 2. Strikingly, control flies showed a clear preference for lactic acid over the other acids; however, this preference was completely abolished in *IR25a* mutants, which consumed equal amounts of lactic acid and either acetic or propionic acid (Figures 7B and S6C). Moreover, calcium imaging showed that the increased sensitivity to lactic acid over other acids is eliminated in *IR25a* mutants (Figure 7C).

Consistent with their behavior toward lactic acid,  $\Delta$ *Gr64a-f* mutants lose much of their feeding preference for acetic and propionic acid (Figure 7D). However, in contrast with *IR25a* mutants,  $\Delta$ *Gr64a-f* mutants retained preference for lactic acid over the other acids in the pH-matched choice assay (Figure 7E). Although

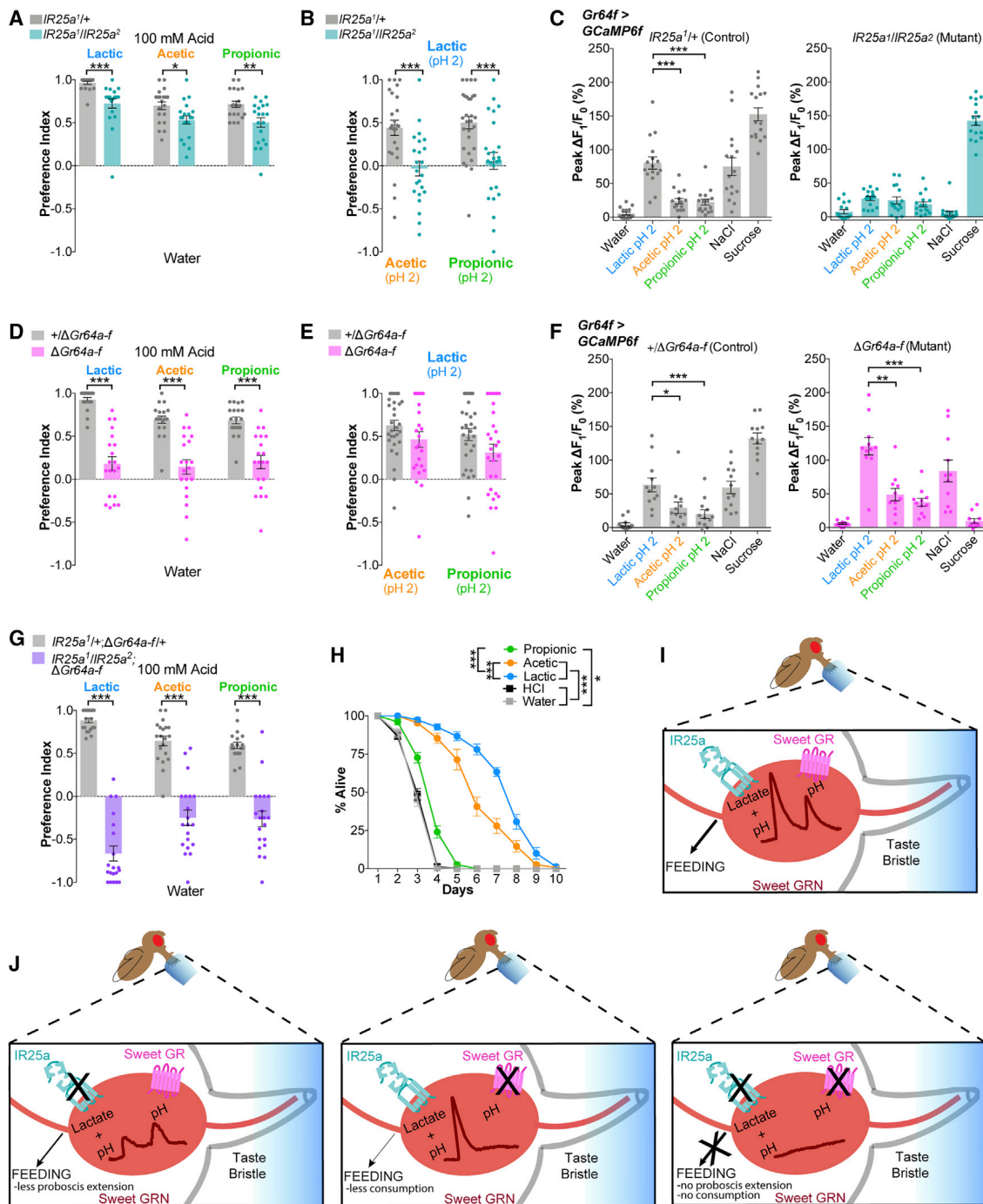


**Figure 7. Differentiation between lactic and other attractive acids requires IR25a**

(A) Feeding preference of  $IR25a$  mutants for indicated acid over water.  $n = 20$  groups of 10 flies.

(B) Feeding preference of  $IR25a$  mutants for lactic acid over indicated acid in a volume-based assay with pH-matched, 200 mM solutions.  $n = 23$ –29 groups of 10 flies.

(C) Sweet GRN calcium imaging in  $IR25a$  mutants with pH-matched solutions, showing peak onset fluorescence changes.  $n = 16$  flies.

(D) Feeding preference of  $\Delta Gr64a-f$  mutants for indicated acid over water.  $n = 20$  groups of 10 flies.

(E) Feeding preference of  $\Delta Gr64a-f$  mutants for lactic acid over indicated acid in a volume-based assay with pH-matched, 200 mM solutions.  $n = 24$ –31 groups of 10 flies.

(F) Sweet GRN calcium imaging in  $\Delta Gr64a-f$  mutants with pH-matched solutions, showing peak onset fluorescence changes.  $n = 11$ –12 flies.

(G) Feeding preference of  $IR25a$ ,  $\Delta Gr64a-f$  combined mutants for indicated acid over water.  $n = 20$  groups of 10 flies.

All bars represent mean  $\pm$  SEM. Asterisks indicate significant differences by two-way ANOVA with Sidak's post-test (A, B, D, and G) or one-way ANOVA with Dunnett's post-test (C and F). See [Figure S6](#).

(legend continued on next page)

to bitter compounds.<sup>38,39</sup> For bitter, the same receptors mediate both onset and removal and the distinct peaks are propagated to higher order taste circuits.<sup>38,39</sup> Our analysis suggests that both onset and removal peaks in sweet GRNs positively contribute to specific, attractive feeding behaviors. We do not know how the loss of removal responses leads to lower acid consumption, but we suspect that the removal peak may promote re-engagement with the food. Future investigation into how taste circuits encode the temporal aspects of taste stimuli will shed light on how the timing of responses impacts appetitive feeding programs.

In *Drosophila*, two techniques are commonly used to assess GRN activation by tastants: calcium imaging of molecularly defined populations of neurons, and single sensillum electrophysiology (tip recordings). While these two methods have largely led to similar conclusions, each has its own strengths. Among other differences, calcium imaging allows visualization of activity before, during, and after stimulation, which is necessary to observe removal responses.<sup>38,39</sup> On the other hand, tip recordings report activity in individual sensilla, and recordings of L-type sensilla have not been found to respond to acid stimulation alone.<sup>10,15</sup> Given the heterogeneity in sweet GRN projection responses during stimulus onset and removal, it is possible that acids stimulate a subset of sweet GRNs outside of those measured in tip recordings.<sup>5,35</sup>

The heterogeneity between IR56d+ and IR56d– sweet neurons also has potential implications for the contributions of individual sweet GRs to acid responses and the behavioral relevance of each neuron subset. Because IR56d+ neurons appear primarily housed in I- and L-type sensilla<sup>40</sup> and each sensillar type has slightly different GR expression profiles,<sup>41</sup> it is possible that differences in GR composition or dose underlie the difference in acid responses. Alternatively, perhaps presynaptic inhibition of sweet GRN axon terminals by bitter neuron activation<sup>42</sup> is more prominent in the IR56d+ synaptic regions. It will be interesting to investigate whether IR56d+ and IR56d– postsynaptic circuits differentially impact feeding behavior and contribute to the greater role of onset and removal responses in proboscis extension and consumption, respectively.

### A dual receptor mechanism in gustatory acid attraction

To our knowledge, this is the first instance where gustatory detection of a single compound requires two different receptor families, IRs and GRs, working in concert. IR25a appears to primarily mediate the onset peak, which correlates with proboscis extension, and is likely driven by the specific anion. Conversely, sweet GRs appear to dampen this onset peak. These GRs also mediate the removal peak, which is a non-specific low-pH response that correlates with ingestion. One curious observation is that *IR25a* mutants retain a small onset peak and  $\Delta$ *Gr64a-f* mutants have enhanced onset, yet the combined mutants show no response at all. We speculate that GRs and IR25a both respond to onset of low pH to some extent, and in the

absence of GRs, enhancement of IR25a-dependent activity masks loss of the small GR-dependent onset response.

We were surprised that IR76b did not contribute to lactic acid attraction, given its overlapping functions with IR25a in chemoreception.<sup>5,25,30–32</sup> Instead, it appears to be involved in limiting lactic acid attraction. Both IRs are expressed broadly across many classes of GRNs on the labellum,<sup>5,30</sup> and we cannot rule out that they are contributing to the detection of acids in bitter GRNs. However, the results with *IR76b* mutants fits with a proposed role for IR76b in limiting sensitivity directly in sweet GRNs.<sup>43</sup>

The involvement of sweet GRs in acid attraction was also surprising. *Drosophila melanogaster* has nine known sweet GRs, which are well characterized in their detection of specific sugars.<sup>33–36,44–46</sup> Similar to IRs, these GRs are thought to function as multimers, with Gr64f being a possible co-receptor for sugar detection.<sup>34</sup> Recently, Gr64e, which acts as a glycerol receptor, was also shown to have a non-canonical role in fatty acid taste transduction downstream of phospholipase C (PLC).<sup>47</sup> Thus, a single GR can act as both an ionotropic chemoreceptor and indirectly contribute to the detection of other molecules. However, acetic acid taste is PLC independent, and the same is likely true for lactic acid.<sup>24</sup>

Our data suggesting that all nine sugar GRs contribute to lactic acid feeding were unexpected but likely reflect dose sensitivity and the non-specific nature of GR acid responses. Notably, bitter GRNs express a large complement of GRs and are also generally acid sensitive.<sup>10,48–50</sup> We speculate that, in sweet GRNs at rest, GRs are in a configuration that either limits the amount of acid entering the cell or limits the response of IR25a to low pH. With sufficient acidification of the lymph and/or intracellular fluid, the gating or conformation of GRs may change so that relief from acidity results in additional ion flux. Although the acid removal peak is most prominent at high concentrations, we suspect it is present at lower concentrations, but the limitations of our GCaMP imaging make these small responses insignificant in the context of the falling onset peak. Moreover, while only high concentrations produce a large-enough resolvable removal peak to observe a significant reduction in GR mutants, our behavioral analyses indicate that effects likely exist at lower concentrations.

### Lactic acid is a highly attractive chemosensory cue

Our results confirm that lactic acid is particularly attractive to *Drosophila*, more so than other commonly studied carboxylic acids. Surprisingly, lactic acid has not been used in *Drosophila* olfaction studies, despite being a key mosquito attractant.<sup>51</sup> Similar to mosquitoes,<sup>27</sup> we found that lactic acid smell is attractive to *Drosophila* and requires IR8a. Given that IR8a also mediates olfactory acid avoidance,<sup>52</sup> lactic acid likely activates both attractive and aversive olfactory neurons, similar to other acidic stimuli.<sup>53</sup> Removing olfactory organs had no impact on lactic acid feeding attraction, whereas *IR8a* mutants had a small but significant reduction in feeding preference. These results

(H) Survival of *w<sup>1118</sup>* flies on 250 mM indicated acids or HCl pH = 2. Points represent mean  $\pm$  SEM; n = 15 groups of 10 flies. Asterisks signify significance by two-way ANOVA with Tukey's post-test. All significance denoted as \*p < 0.05, \*\*p < 0.01, and \*\*\*p < 0.001.

(I) Model of a sweet GRN inside a taste sensillum: the onset calcium peak is largely in response to lactate detection by IR25a, and the removal peak is generated by a change in pH via sweet GRs.

(J) Model summarizing how elimination of each receptor type, individually or combined, affects sweet GRN calcium responses and feeding behavior. See Figure S6.

highlight the complexity of the full chemosensory response to lactic acid. Future experiments can further explore the integration of lactic acid taste and smell, including how mosquito lactic acid taste may influence biting.

We briefly explored one potential reason driving attraction to lactic acid in *Drosophila* by investigating its ability to provide energy. Lactic acid was particularly effective in improving fly survival, likely because lactate is a fuel for the TCA cycle.<sup>54</sup> Serving as an energy source was speculated to be one reason for attraction to acetic acid in a previous study,<sup>24</sup> and we find that acetic acid provides energy to flies but less efficiently than lactic acid. Additional explanations, such as attraction to specific gut microbes, undoubtedly also exist.

### STAR★METHODS

Detailed methods are provided in the online version of this paper and include the following:

- KEY RESOURCES TABLE
- RESOURCE AVAILABILITY
  - Lead contact
  - Materials availability
  - Data and code availability
- EXPERIMENTAL MODEL AND SUBJECT DETAILS
  - Flies
- METHOD DETAILS
  - Tastants
  - Behavioral assays
  - Calcium imaging
  - Survival assay
  - Immunohistochemistry
- QUANTIFICATION AND STATISTICAL ANALYSIS

### SUPPLEMENTAL INFORMATION

Supplemental information can be found online at <https://doi.org/10.1016/j.cub.2021.06.005>.

### ACKNOWLEDGMENTS

We thank Anupama Dahanukar, the Bloomington Stock Center, and the Vienna *Drosophila* Resource Center for fly stocks and members of the Gordon lab for comments on the manuscript. This work was funded by the Canadian Institutes of Health Research (CIHR) operating grant FDN-148424. M.D.G. is a Michael Smith Foundation for Health Research Scholar.

### AUTHOR CONTRIBUTIONS

Conceptualization, M.S. and M.D.G.; methodology, M.S. and M.D.G.; formal analysis, M.S.; investigation, M.S., B.G., Z.F.W., and J.C.; resources, M.D.G.; writing – original draft, M.S. and M.D.G.; writing – review & editing, M.S., B.G., and M.D.G.; visualization, M.S.; supervision, M.D.G.; funding acquisition, M.D.G.

### DECLARATION OF INTERESTS

The authors declare no competing interests.

Received: February 10, 2021

Revised: April 30, 2021

Accepted: June 2, 2021

Published: June 30, 2021

### REFERENCES

1. Behrens, M., Blank, K., and Meyerhof, W. (2017). Blends of non-caloric sweeteners saccharin and cyclamate show reduced off-taste due to TAS2R bitter receptor inhibition. *Cell Chem. Biol.* 24, 1199–1204.e2.
2. Chandrashekar, J., Kuhn, C., Oka, Y., Yarmolinsky, D.A., Hummler, E., Ryba, N.J.P., and Zuker, C.S. (2010). The cells and peripheral representation of sodium taste in mice. *Nature* 464, 297–301.
3. Freeman, E.G., Wisotsky, Z., and Dahanukar, A. (2014). Detection of sweet tastants by a conserved group of insect gustatory receptors. *Proc. Natl. Acad. Sci. USA* 111, 1598–1603.
4. French, A.S., Sellier, M.-J., Ali Agha, M., Guigue, A., Chabaud, M.-A., Reeb, P.D., Mitra, A., Grau, Y., Soustelle, L., and Marion-Poll, F. (2015). Dual mechanism for bitter avoidance in *Drosophila*. *J. Neurosci.* 35, 3990–4004.
5. Jaeger, A.H., Stanley, M., Weiss, Z.F., Musso, P.-Y., Chan, R.C., Zhang, H., Feldman-Kiss, D., and Gordon, M.D. (2018). A complex peripheral code for salt taste in *Drosophila*. *eLife* 7, e37167.
6. Jeong, Y.T., Shim, J., Oh, S.R., Yoon, H.I., Kim, C.H., Moon, S.J., and Montell, C. (2013). An odorant-binding protein required for suppression of sweet taste by bitter chemicals. *Neuron* 79, 725–737.
7. Meunier, N., Marion-Poll, F., Rospars, J.-P., and Tanimura, T. (2003). Peripheral coding of bitter taste in *Drosophila*. *J. Neurobiol.* 56, 139–152.
8. Roebber, J.K., Roper, S.D., and Chaudhari, N. (2019). The role of the anion in salt (NaCl) detection by mouse taste buds. *J. Neurosci.* 39, 6224–6232.
9. Zhang, J., Jin, H., Zhang, W., Ding, C., O’Keeffe, S., Ye, M., and Zuker, C.S. (2019). Sour sensing from the tongue to the brain. *Cell* 179, 392–402.e15.
10. Charlu, S., Wisotsky, Z., Medina, A., and Dahanukar, A. (2013). Acid sensing by sweet and bitter taste neurons in *Drosophila melanogaster*. *Nat. Commun.* 4, 2042.
11. Wang, Y.Y., Chang, R.B., Allgood, S.D., Silver, W.L., and Liman, E.R. (2011). A TRPA1-dependent mechanism for the pungent sensation of weak acids. *J. Gen. Physiol.* 137, 493–505.
12. Chang, R.B., Waters, H., and Liman, E.R. (2010). A proton current drives action potentials in genetically identified sour taste cells. *Proc. Natl. Acad. Sci. USA* 107, 22320–22325.
13. Ai, M., Min, S., Grosjean, Y., Leblanc, C., Bell, R., Benton, R., and Suh, G.S.B. (2010). Acid sensing by the *Drosophila* olfactory system. *Nature* 468, 691–695.
14. Depetris-Chauvin, A., Galagovsky, D., Chevalier, C., Maniere, G., and Grosjean, Y. (2017). Olfactory detection of a bacterial short-chain fatty acid acts as an orexigenic signal in *Drosophila melanogaster* larvae. *Sci. Rep.* 7, 14230.
15. Rimal, S., Sang, J., Poudel, S., Thakur, D., Montell, C., and Lee, Y. (2019). Mechanism of acetic acid gustatory repulsion in *Drosophila*. *Cell Rep.* 26, 1432–1442.e4.
16. Huang, A.L., Chen, X., Hoon, M.A., Chandrashekar, J., Guo, W., Tränkner, D., Ryba, N.J.P., and Zuker, C.S. (2006). The cells and logic for mammalian sour taste detection. *Nature* 442, 934–938.
17. Teng, B., Wilson, C.E., Tu, Y.-H., Joshi, N.R., Kinnamon, S.C., and Liman, E.R. (2019). Cellular and neural responses to sour stimuli require the proton channel Otop1. *Curr. Biol.* 29, 3647–3656.e5.
18. Tu, Y.-H., Cooper, A.J., Teng, B., Chang, R.B., Artiga, D.J., Turner, H.N., Mulhall, E.M., Ye, W., Smith, A.D., and Liman, E.R. (2018). An evolutionarily conserved gene family encodes proton-selective ion channels. *Science* 359, 1047–1050.
19. Ramos Da Conceicao Neta, E.R., Johanningsmeier, S.D., and McFeeters, R.F. (2007). The chemistry and physiology of sour taste—a review. *J. Food Sci.* 72, R33–R38.
20. Harvey, R.B. (1920). The relationship between the total acidity, the concentration of the hydrogen ion, and the taste of acid solutions. *J. Am. Chem. Soc.* 42, 712–714.



21. Pfeiffer, J.C., Hort, J., Hollowood, T.A., and Taylor, A.J. (2006). Taste-aroma interactions in a ternary system: a model of fruitiness perception in sucrose/acid solutions. *Percept. Psychophys.* *68*, 216–227.
22. Deshpande, S.A., Yamada, R., Mak, C.M., Hunter, B., Soto Obando, A., Hoxha, S., and Ja, W.W. (2015). Acidic food pH increases palatability and consumption and extends *Drosophila* lifespan. *J. Nutr.* *145*, 2789–2796.
23. Qiao, H., Keeseey, I.W., Hansson, B.S., and Knaden, M. (2019). Gut microbiota affects development and olfactory behavior in *Drosophila melanogaster*. *J. Exp. Biol.* *222*, jeb192500.
24. Devineni, A.V., Sun, B., Zhukovskaya, A., and Axel, R. (2019). Acetic acid activates distinct taste pathways in *Drosophila* to elicit opposing, state-dependent feeding responses. *eLife* *8*, e47677.
25. Chen, Y., and Amrein, H. (2017). Ionotropic receptors mediate *Drosophila* oviposition preference through sour gustatory receptor neurons. *Curr. Biol.* *27*, 2741–2750.e4.
26. Massie, H.R., and Williams, T.R. (1979). Increased longevity of *Drosophila melanogaster* with lactic and gluconic acids. *Exp. Gerontol.* *14*, 109–115.
27. Raji, J.I., Melo, N., Castillo, J.S., Gonzalez, S., Saldana, V., Stensmyr, M.C., and DeGennaro, M. (2019). *Aedes aegypti* mosquitoes detect acidic volatiles found in human odor using the IR8a pathway. *Curr. Biol.* *29*, 1253–1262.e7.
28. Menuz, K., Larter, N.K., Park, J., and Carlson, J.R. (2014). An RNA-seq screen of the *Drosophila* antenna identifies a transporter necessary for ammonia detection. *PLoS Genet.* *10*, e1004810.
29. Tauber, J.M., Brown, E.B., Li, Y., Yurgel, M.E., Masek, P., and Keene, A.C. (2017). A subset of sweet-sensing neurons identified by IR56d are necessary and sufficient for fatty acid taste. *PLoS Genet.* *13*, e1007059.
30. Lee, Y., Poudel, S., Kim, Y., Thakur, D., and Montell, C. (2018). Calcium taste avoidance in *Drosophila*. *Neuron* *97*, 67–74.e4.
31. Ahn, J.-E., Chen, Y., and Amrein, H. (2017). Molecular basis of fatty acid taste in *Drosophila*. *eLife* *6*, e30115.
32. Sánchez-Alcañiz, J.A., Silbering, A.F., Croset, V., Zappia, G., Sivasubramanian, A.K., Abuin, L., Sahai, S.Y., Münch, D., Steck, K., Auer, T.O., et al. (2018). An expression atlas of variant ionotropic glutamate receptors identifies a molecular basis of carbonation sensing. *Nat. Commun.* *9*, 4252.
33. Yavuz, A., Jagge, C., Slone, J., and Amrein, H. (2014). A genetic tool kit for cellular and behavioral analyses of insect sugar receptors. *Fly (Austin)* *8*, 189–196.
34. Jiao, Y., Moon, S.J., Wang, X., Ren, Q., and Montell, C. (2008). Gr64f is required in combination with other gustatory receptors for sugar detection in *Drosophila*. *Curr. Biol.* *18*, 1797–1801.
35. Dahanukar, A., Lei, Y.-T., Kwon, J.Y., and Carlson, J.R. (2007). Two Gr genes underlie sugar reception in *Drosophila*. *Neuron* *56*, 503–516.
36. Miyamoto, T., Slone, J., Song, X., and Amrein, H. (2012). A fructose receptor functions as a nutrient sensor in the *Drosophila* brain. *Cell* *151*, 1113–1125.
37. Holzer, P. (2009). Acid-sensitive ion channels and receptors. In *Sensory Nerves Handbook of Experimental Pharmacology*, B.J. Canning, and D. Spina, eds. (Springer Berlin Heidelberg), pp. 283–332.
38. Devineni, A.V., Deere, J.U., Sun, B., and Axel, R. (2020). Individual bitter-sensing neurons in *Drosophila* exhibit both ON and OFF responses that influence synaptic plasticity. *bioRxiv*. <https://doi.org/10.1101/2020.08.25.266619>.
39. Snell, N.J., Fisher, J.D., Hartmann, G.G., Talay, M., and Barnea, G. (2020). Distributed representation of taste quality by second-order gustatory neurons in *Drosophila*. *bioRxiv*. <https://doi.org/10.1101/2020.11.10.377382>.
40. Koh, T.-W., He, Z., Gorur-Shandilya, S., Menuz, K., Larter, N.K., Stewart, S., and Carlson, J.R. (2014). The *Drosophila* IR20a clade of ionotropic receptors are candidate taste and pheromone receptors. *Neuron* *83*, 850–865.
41. Fujii, S., Yavuz, A., Slone, J., Jagge, C., Song, X., and Amrein, H. (2015). *Drosophila* sugar receptors in sweet taste perception, olfaction, and internal nutrient sensing. *Curr. Biol.* *25*, 621–627.
42. Chu, B., Chui, V., Mann, K., and Gordon, M.D. (2014). Presynaptic gain control drives sweet and bitter taste integration in *Drosophila*. *Curr. Biol.* *24*, 1978–1984.
43. Chen, H.-L., Stern, U., and Yang, C.-H. (2019). Molecular control limiting sensitivity of sweet taste neurons in *Drosophila*. *Proc. Natl. Acad. Sci. USA* *116*, 20158–20168.
44. Slone, J., Daniels, J., and Amrein, H. (2007). Sugar receptors in *Drosophila*. *Curr. Biol.* *17*, 1809–1816.
45. Dahanukar, A., Foster, K., van der Goes van Naters, W.M., and Carlson, J.R. (2001). A Gr receptor is required for response to the sugar trehalose in taste neurons of *Drosophila*. *Nat. Neurosci.* *4*, 1182–1186.
46. Wisotsky, Z., Medina, A., Freeman, E., and Dahanukar, A. (2011). Evolutionary differences in food preference rely on Gr64e, a receptor for glycerol. *Nat. Neurosci.* *14*, 1534–1541.
47. Kim, H., Kim, H., Kwon, J.Y., Seo, J.T., Shin, D.M., and Moon, S.J. (2018). *Drosophila* Gr64e mediates fatty acid sensing via the phospholipase C pathway. *PLoS Genet.* *14*, e1007229.
48. Thorne, N., Chromey, C., Bray, S., and Amrein, H. (2004). Taste perception and coding in *Drosophila*. *Curr. Biol.* *14*, 1065–1079.
49. Wang, Z., Singhvi, A., Kong, P., and Scott, K. (2004). Taste representations in the *Drosophila* brain. *Cell* *117*, 981–991.
50. Weiss, L.A., Dahanukar, A., Kwon, J.Y., Banerjee, D., and Carlson, J.R. (2011). The molecular and cellular basis of bitter taste in *Drosophila*. *Neuron* *69*, 258–272.
51. McBride, C.S. (2016). Genes and odors underlying the recent evolution of mosquito preference for humans. *Curr. Biol.* *26*, R41–R46.
52. Ai, M., Blais, S., Park, J.-Y., Min, S., Neubert, T.A., and Suh, G.S.B. (2013). Ionotropic glutamate receptors IR64a and IR8a form a functional odorant receptor complex in vivo in *Drosophila*. *J. Neurosci.* *33*, 10741–10749.
53. Semmelhack, J.L., and Wang, J.W. (2009). Select *Drosophila* glomeruli mediate innate olfactory attraction and aversion. *Nature* *459*, 218–223.
54. Rabinowitz, J.D., and Enerbäck, S. (2020). Lactate: the ugly duckling of energy metabolism. *Nat. Metab.* *2*, 566–571.
55. Baines, R.A., Uhler, J.P., Thompson, A., Sweeney, S.T., and Bate, M. (2001). Altered electrical properties in *Drosophila* neurons developing without synaptic transmission. *J. Neurosci.* *21*, 1523–1531.
56. McGuire, S.E., Mao, Z., and Davis, R.L. (2004). Spatiotemporal gene expression targeting with the TARGET and gene-switch systems in *Drosophila*. *Sci. STKE* *2004*, pl6.
57. Tirian, L., and Dickson, B.J. (2017). The VT GAL4, LexA, and split-GAL4 driver line collections for targeted expression in the *Drosophila* nervous system. *bioRxiv*. <https://doi.org/10.1101/198648>.
58. Thistle, R., Cameron, P., Ghorayshi, A., Dennison, L., and Scott, K. (2012). Contact chemoreceptors mediate male-male repulsion and male-female attraction during *Drosophila* courtship. *Cell* *149*, 1140–1151.
59. Cameron, P., Hiroi, M., Ngai, J., and Scott, K. (2010). The molecular basis for water taste in *Drosophila*. *Nature* *465*, 91–95.
60. Benton, R., Vannice, K.S., Gomez-Diaz, C., and Vosshall, L.B. (2009). Variant ionotropic glutamate receptors as chemosensory receptors in *Drosophila*. *Cell* *136*, 149–162.
61. Zhang, Y.V., Ni, J., and Montell, C. (2013). The molecular basis for attractive salt-taste coding in *Drosophila*. *Science* *340*, 1334–1338.
62. Uchizono, S., Itoh, T.Q., Kim, H., Hamada, N., Kwon, J.Y., and Tanimura, T. (2017). Deciphering the genes for taste receptors for fructose in *Drosophila*. *Mol. Cells* *40*, 731–736.
63. Kwon, J.Y., Dahanukar, A., Weiss, L.A., and Carlson, J.R. (2011). Molecular and cellular organization of the taste system in the *Drosophila* larva. *J. Neurosci.* *31*, 15300–15309.
64. Schneider, C.A., Rasband, W.S., and Eliceiri, K.W. (2012). NIH Image to ImageJ: 25 years of image analysis. *Nat. Methods* *9*, 671–675.

65. Ogueta, M., Cibik, O., Eltrop, R., Schneider, A., and Scholz, H. (2010). The influence of Adh function on ethanol preference and tolerance in adult *Drosophila melanogaster*. *Chem. Senses* 35, 813–822.
66. Stensmyr, M.C., Dweck, H.K.M., Farhan, A., Ibba, I., Strutz, A., Mukunda, L., Linz, J., Grabe, V., Steck, K., Lavista-Llanos, S., et al. (2012). A conserved dedicated olfactory circuit for detecting harmful microbes in *Drosophila*. *Cell* 151, 1345–1357.
67. Stafford, J.W., Lynd, K.M., Jung, A.Y., and Gordon, M.D. (2012). Integration of taste and calorie sensing in *Drosophila*. *J. Neurosci.* 32, 14767–14774.

STAR★METHODS

KEY RESOURCES TABLE

REAGENT or RESOURCE	SOURCE	IDENTIFIER
<b>Antibodies</b>		
Mouse anti-brp	DSHB	Nc82; RRID: AB_2392664
Rabbit anti-GFP	Invitrogen	Cat#A11122; RRID: AB_221569
Anti-rabbit Alexa 488	Invitrogen	Cat#A11008; RRID: AB_143165
Anti-mouse Alexa 546	Invitrogen	Cat#A11030; RRID: AB_144695
<b>Chemicals, peptides, and recombinant proteins</b>		
DL-Lactic Acid	Sigma-Aldrich	Cat#69785
Sucrose	Sigma-Aldrich	Cat#S7903
NaCl	Sigma-Aldrich	Cat#S7653
Caffeine	Sigma-Aldrich	Cat#C0750
NaOH	Sigma-Aldrich	Cat#1310-23-10
Acetic Acid	Sigma-Aldrich	Cat#64-19-7
Propionic Acid	Sigma-Aldrich	Cat#79-09-4
Hydrochloric Acid	Sigma-Aldrich	Cat#351280-212
Agar	Sigma-Aldrich	Cat#A1296
Erioglaucine, FD&C Blue #1	Spectrum	Cat#FD110
Amaranth FD&C Red #2	Sigma-Aldrich	Cat#A1016
4% Paraformaldehyde in PBS	Alfa Aesar	Cat#J61899
<b>Deposited data</b>		
Raw data from all Figures	Mendeley Data	<a href="https://dx.doi.org/10.17632/2jc6fbjkkx.1">https://dx.doi.org/10.17632/2jc6fbjkkx.1</a>
<b>Experimental models: organisms/strains</b>		
<i>D. melanogaster: w<sup>1118</sup></i>	Bloomington Drosophila Stock Center	BDSC: 3605; RRID: BDSC_3605
<i>D. melanogaster: Canton S.</i>	Bloomington Drosophila Stock Center	BDSC: 64349; RRID: BDSC_64349
<i>D. melanogaster: IR8a<sup>1</sup></i>	Bloomington Drosophila Stock Center	BDSC: 41744; RRID: BDSC_41744
<i>D. melanogaster: UAS-Kir2.1</i>	Baines et al. <sup>55</sup>	Flybase: FBti0017552
<i>D. melanogaster: Tub-Gal80<sup>TS</sup></i>	McGuire et al. <sup>56</sup>	Flybase: FBti0027797
<i>D. melanogaster: Ir94e-Gal4</i>	Jaeger et al. <sup>5</sup> and Tirian and Dickson <sup>57</sup>	VDR: v207582
<i>D. melanogaster: Gr66a-LexA</i>	Thistle et al. <sup>58</sup>	Flybase: FBal0277069
<i>D. melanogaster: LexAop-Gal80</i>	Bloomington Drosophila Stock Center	BDSC: 44277; RRID: BDSC_44277
<i>D. melanogaster: Ppk28-Gal4</i>	Cameron et al. <sup>59</sup>	Flybase: FBtp0054514
<i>D. melanogaster: Gr66a-Gal4</i>	Wang et al. <sup>49</sup>	Flybase: FBtp0014660
<i>D. melanogaster: Gr64f-Gal4</i>	Dahanukar et al. <sup>35</sup>	Flybase: FBti0162678
<i>D. melanogaster: Gr64f-Gal4</i>	Dahanukar et al. <sup>35</sup>	Flybase: FBtp0057275
<i>D. melanogaster: IR56d-Gal4</i>	Sánchez-Alcañiz et al. <sup>32</sup>	BDSC: 81235; RRID: BDSC_81235
<i>D. melanogaster: UAS-GCaMP6f</i>	Bloomington Drosophila Stock Center	BDSC: 42747; RRID: BDSC_42747
<i>D. melanogaster: UAS-GCaMP6f</i>	Bloomington Drosophila Stock Center	BDSC: 52869; RRID: BDSC_52869
<i>D. melanogaster: IR25a<sup>1</sup></i>	Benton et al. <sup>60</sup>	Flybase: FBst0041736
<i>D. melanogaster: IR25a<sup>2</sup></i>	Benton et al. <sup>60</sup>	Flybase: FBst0041737
<i>D. melanogaster: UAS-IR25a</i>	Bloomington Drosophila Stock Center	BDSC: 78067; RRID: BDSC_78067
<i>D. melanogaster: IR76b<sup>1</sup></i>	Zhang et al. <sup>61</sup>	Flybase: FBst0051309
<i>D. melanogaster: IR76b<sup>2</sup></i>	Zhang et al. <sup>61</sup>	Flybase: FBst0051310
<i>D. melanogaster: ΔIR62a</i>	Bloomington Drosophila Stock Center	BDSC: 32713; RRID: BDSC_32713
<i>D. melanogaster: IR56b<sup>GAL4</sup></i>	Bloomington Drosophila Stock Center	BDSC: 27818; RRID: BDSC_27818
<i>D. melanogaster: UAS-IR56d<sup>RNAi</sup></i>	Vienna Drosophila Resource Center	VDR: 6112
<i>D. melanogaster: UAS-IR7c<sup>RNAi</sup></i>	Vienna Drosophila Resource Center	VDR: 109485

(Continued on next page)

**Continued**

REAGENT or RESOURCE	SOURCE	IDENTIFIER
<i>D. melanogaster</i> : $\Delta$ Gr5a	Dahanukar et al. <sup>45</sup>	Flybase: FBal0127256
<i>D. melanogaster</i> : Gr43a <sup>GAL4</sup>	Miyamoto et al. <sup>36</sup>	Flybase: FBal0290232
<i>D. melanogaster</i> : $\Delta$ Gr61a <sup>1</sup>	Dahanukar et al. <sup>35</sup>	Flybase: FBal0256895
<i>D. melanogaster</i> : $\Delta$ Gr64a <sup>1</sup>	Dahanukar et al. <sup>35</sup>	Flybase: FBal0256892
<i>D. melanogaster</i> : $\Delta$ Gr64a <sup>2</sup>	Dahanukar et al. <sup>35</sup>	Flybase: FBab0047074
<i>D. melanogaster</i> : $\Delta$ Gr64d <sup>1</sup>	Uchizono et al. <sup>62</sup>	Flybase: FBal0346605
<i>D. melanogaster</i> : $\Delta$ Gr64e <sup>MB03533</sup>	Wisotsky et al. <sup>46</sup>	Flybase: FBal0192448
<i>D. melanogaster</i> : Gr64f <sup>EXA</sup>	Yavuz et al. <sup>33</sup>	Flybase: FBal0304291
<i>D. melanogaster</i> : $\Delta$ Gr64a-f	Kim et al. <sup>47</sup>	Flybase: FBab0049044
<i>D. melanogaster</i> : R1,Gr5a <sup>LEXA</sup> ;; $\Delta$ Gr61a, $\Delta$ Gr64a-f	Yavuz et al. <sup>33</sup>	Flybase: FBal0304286 Fbal0256895 Fbab0047080
<i>D. melanogaster</i> : Gr64e-Gal4	Kwon et al. <sup>63</sup>	BDSC: 57666; RRID: BDSC_57666
<i>D. melanogaster</i> : UAS-mCD8::GFP	Bloomington Drosophila Stock Center	BDSC: 32195; RRID: BDSC_32195
<b>Software and algorithms</b>		
ImageJ	Schneider et al. <sup>64</sup>	RRID: SCR_003070
Prism 6	Graphpad	RRID: SCR_002798
Illustrator	Adobe	RRID: SCR_010279

**RESOURCE AVAILABILITY**

**Lead contact**

Requests for resources, reagents, and further information should be directed to and will be fulfilled by Michael Gordon ([gordon@zoology.ubc.ca](mailto:gordon@zoology.ubc.ca)).

**Materials availability**

This study did not generate new unique reagents.

**Data and code availability**

All raw numerical data from Figures were deposited on Mendeley at <https://dx.doi.org/10.17632/2jc6fbjkkx.1>

**EXPERIMENTAL MODEL AND SUBJECT DETAILS**

**Flies**

*Drosophila melanogaster* of indicated genotypes were raised on standard cornmeal fly food at 25°C in 70% humidity. All experiments were performed on 2-10 day-old adult flies. Mated females were used unless stated otherwise where sex and mating status were tested in the main behavioral assay. Genotypes used in each experiment are listed below, additional source and strain information can be found in the [Key resources table](#).

Figure 1:

- *w*<sup>1118</sup>
- *Ir8a*<sup>1</sup>/+; +/+; +/+
- *Ir8a*<sup>1</sup>/*Ir8a*<sup>1</sup>; +/+; +/+

Figure 2:

- +/+; +/+; UAS-Kir2.1,tub-Gal80<sup>TS</sup>/+
- +/+; Gr64f-Gal4/+; +/+
- +/+; Gr64f-Gal4/+; UAS-Kir2.1,tub-Gal80<sup>TS</sup>/+
- +/+; +/+; *Ir94e*-Gal4/+
- +/+; +/+; *Ir94e*-Gal4/UAS-Kir2.1,tubGal80<sup>TS</sup>
- Gr66a-LexA/+; LexAop-Gal80/+; Ppk23-Gal4/+
- Gr66a-LexA/+; LexAop-Gal80/+; Ppk23-Gal4/UAS-Kir2.1,tub-Gal80<sup>TS</sup>



- +/+; +/+; *Ppk28-Gal4/+*
- +/+; +/+; *Ppk28-Gal4/UAS-Kir2.1,tub-Gal80<sup>TS</sup>*
- +/+; *Gr66a-Gal4/+*; +/+
- +/+; *Gr66a-Gal4/+*; *UAS-Kir2.1,tub-Gal80<sup>TS</sup>/+*
- +/+; *Gr64f-Gal4/UAS-GCaMP6f*; +/+
- +/+; *IR56d-Gal4/UAS-GCaMP6f*; +/+

Figure 3:

- +/+; *Gr64f-Gal4/UAS-GCaMP6f*; +/+

Figure 4:

- +/+; *IR25a<sup>1</sup>/+*; +/+
- +/+; *IR25a<sup>2</sup>/+*; +/+
- +/+; *IR25a<sup>1</sup>/IR25a<sup>2</sup>*; +/+
- +/+; *IR25a<sup>1</sup>/+*; *UAS-IR25a/+*
- +/+; *IR25a<sup>2</sup>/+*; *Gr64f-Gal4/+*
- +/+; *IR25a<sup>1</sup>/IR25a<sup>2</sup>*; *UAS-IR25a/+*
- +/+; *IR25a<sup>1</sup>/IR25a<sup>2</sup>*; *Gr64f-Gal4/+*
- +/+; *IR25a<sup>1</sup>/IR25a<sup>2</sup>*; *Gr64f-Gal4/UAS-IR25a*
- +/+; +/+; *IR76b<sup>1</sup>/+*
- +/+; +/+; *IR76b<sup>2</sup>/+*
- +/+; +/+; *IR76b<sup>1</sup>/IR76b<sup>2</sup>*
- +/+; *IR25a<sup>1</sup>/+*; *Gr64f-Gal4/UAS-GCaMP6f*
- +/+; *IR25a<sup>1</sup>/IR25a<sup>2</sup>*; *Gr64f-Gal4/UAS-GCaMP6f*
- +/+; *IR25a<sup>1</sup>,UAS-IR25a/IR25a<sup>2</sup>*; *Gr64f-Gal4/UAS-GCaMP6f*

Figure 5:

- $\Delta$ *Gr5a/+*; +/+; +/+
- $\Delta$ *Gr5a/*  $\Delta$ *Gr5a*; +/+; +/+
- +/+; *Gr43a<sup>GAL4</sup>/+*; +/+
- +/+; *Gr43a<sup>GAL4</sup>/Gr43a<sup>GAL4</sup>*; +/+
- +/+;  $\Delta$ *Gr61a<sup>1</sup>/+*; +/+
- +/+;  $\Delta$ *Gr61a<sup>1</sup>/ $\Delta$ *Gr61a<sup>1</sup>*; +/+*
- +/+;  $\Delta$ *Gr64a<sup>1</sup>/+*; +/+
- +/+;  $\Delta$ *Gr64a<sup>1</sup>/ $\Delta$ *Gr64a<sup>1</sup>*; +/+*
- +/+;  $\Delta$ *Gr64a<sup>2</sup>/+*; +/+
- +/+;  $\Delta$ *Gr64a<sup>2</sup>/ $\Delta$ *Gr64a<sup>2</sup>*; +/+*
- +/+;  $\Delta$ *Gr64d<sup>1</sup>/+*; +/+
- +/+;  $\Delta$ *Gr64d<sup>1</sup>/ $\Delta$ *Gr64d<sup>1</sup>*; +/+*
- +/+;  $\Delta$ *Gr64e<sup>MB03533</sup>/+*; +/+
- +/+;  $\Delta$ *Gr64e<sup>MB03533</sup>/ $\Delta$ *Gr64e<sup>MB03533</sup>*; +/+*
- +/+; +/+; *Gr64f<sup>LEXA</sup>/+*
- +/+; +/+; *Gr64f<sup>LEXA</sup>/Gr64f<sup>LEXA</sup>*
- +/+; +/+;  $\Delta$ *Gr64a-f/+*
- +/+; +/+;  $\Delta$ *Gr64a-f/ $\Delta$ *Gr64a-f**
- $\Delta$ *Gr5a/+*;  $\Delta$ *Gr64a/+*; +/+
- $\Delta$ *Gr5a/ $\Delta$ *Gr5a*;  $\Delta$ *Gr64a/ $\Delta$ *Gr64a*; +/+**
- *R1,Gr5a<sup>LEXA</sup>/+*; +/+;  $\Delta$ *Gr61a*,  $\Delta$ *Gr64a-f/+*
- *R1,Gr5a<sup>LEXA</sup>/**R1,Gr5a<sup>LEXA</sup>*; +/+;  $\Delta$ *Gr61a*,  $\Delta$ *Gr64a-f/ $\Delta$ *Gr61a*,  $\Delta$ *Gr64a-f**
- *R1,Gr5a<sup>LEXA</sup>/+*; *Gr43a<sup>GAL4</sup>/+*;  $\Delta$ *Gr61a*,  $\Delta$ *Gr64a-f/+*
- *R1,Gr5a<sup>LEXA</sup>/**R1,Gr5a<sup>LEXA</sup>*; *Gr43a<sup>GAL4</sup>/**Gr43a<sup>GAL4</sup>*;  $\Delta$ *Gr61a*,  $\Delta$ *Gr64a-f/ $\Delta$ *Gr61a*,  $\Delta$ *Gr64a-f**
- +/+; *Gr64f-Gal4,UAS-GCaMP6f/+*;  $\Delta$ *Gr64a-f/+*
- +/+; *Gr64f-Gal4,UAS-GCaMP6f/+*;  $\Delta$ *Gr64a-f/ $\Delta$ *Gr64a-f**

Figure 6:

- +/+; *IR25a<sup>1</sup>,Gr64f-Gal4/UAS-GCaMP6f*;  $\Delta$ *Gr64a-f/+*
- +/+; *IR25a<sup>1</sup>,Gr64f-Gal4/IR25a<sup>2</sup>,UAS-GCaMP6f*;  $\Delta$ *Gr64a-f/ $\Delta$ *Gr64a-f**

- +/+; *IR25a*<sup>1</sup>/+;  $\Delta$ *Gr64a-f*/+
- +/+; *IR25a*<sup>1</sup>/*IR25a*<sup>2</sup>;  $\Delta$ *Gr64a-f*/+
- +/+; *IR25a*<sup>1</sup>/+;  $\Delta$ *Gr64a-f*/ $\Delta$ *Gr64a-f*
- +/+; *IR25a*<sup>1</sup>/*IR25a*<sup>2</sup>;  $\Delta$ *Gr64a-f*/ $\Delta$ *Gr64a-f*

Figure 7:

- +/+; *IR25a*<sup>1</sup>/+; +/+
- +/+; *IR25a*<sup>1</sup>/*IR25a*<sup>2</sup>; +/+
- +/+; *IR25a*<sup>1</sup>/+; *Gr64f-Gal4/UAS-GCaMP6f*
- +/+; *IR25a*<sup>1</sup>/*IR25a*<sup>2</sup>; *Gr64f-Gal4/UAS-GCaMP6f*
- +/+; +/+;  $\Delta$ *Gr64a-f*/+
- +/+; +/+;  $\Delta$ *Gr64a-f*/ $\Delta$ *Gr64a-f*
- +/+; *Gr64f-Gal4,UAS-GCaMP6f*/+;  $\Delta$ *Gr64a-f*/+
- +/+; *Gr64f-Gal4,UAS-GCaMP6f*/+;  $\Delta$ *Gr64a-f*/ $\Delta$ *Gr64a-f*
- +/+; *IR25a*<sup>1</sup>/+;  $\Delta$ *Gr64a-f*/+
- +/+; *IR25a*<sup>1</sup>/*IR25a*<sup>2</sup>;  $\Delta$ *Gr64a-f*/ $\Delta$ *Gr64a-f*

Figure S1:

- *w*<sup>1118</sup>
- Canton S.
- *Ir8a*<sup>1</sup>/+; +/+; +/+
- *Ir8a*<sup>1</sup>/*Ir8a*<sup>1</sup>; +/+; +/+

Figure S2:

- +/+; *Gr64f-Gal4*/+; *UAS-mCD8::GFP*/+
- +/+; +/+; *UAS-Kir2.1,tub-Gal80<sup>TS</sup>*/+
- +/+; *Gr64f-Gal4*/+; +/+
- +/+; *Gr64f-Gal4*/+; *UAS-Kir2.1,tub-Gal80<sup>TS</sup>*/+
- +/+; *Gr64e-Gal4*/+; *UAS-mCD8::GFP*/+
- +/+; +/+; *UAS-Kir2.1,tub-Gal80<sup>TS</sup>*/+
- +/+; *Gr64e-Gal4*/+; +/+
- +/+; *Gr64e-Gal4*/+; *UAS-Kir2.1*/+

Figure S3:

- +/+; *Gr66a-Gal4/UAS-GCaMP6f*; +/+

Figure S4:

- +/+; *Gr64f-Gal4*/+; +/+
- +/+; *Gr64f-Gal4/UAS-Ir7c<sup>RNAi</sup>*; +/+
- +/+; *Gr64f-Gal4*/+; *UAS-IR56d<sup>RNAi</sup>*/+
- +/+; *IR56b<sup>GAL4</sup>*; +/+
- +/+; *IR56b<sup>GAL4</sup>/IR56b<sup>GAL4</sup>*; +/+
- +/+; +/+;  $\Delta$ *IR62a*/ $\Delta$ *IR62a*

Figure S5:

- +/+;  $\Delta$ *Gr61a*<sup>1</sup>/+; +/+
- +/+;  $\Delta$ *Gr61a*<sup>1</sup>/ $\Delta$ *Gr61a*<sup>1</sup>; +/+
- +/+;  $\Delta$ *Gr64d*<sup>1</sup>/+; +/+
- +/+;  $\Delta$ *Gr64d*<sup>1</sup>/ $\Delta$ *Gr64d*<sup>1</sup>; +/+
- +/+; +/+; *Gr64f<sup>LEXA</sup>*/+
- +; +/+; *Gr64f<sup>LEXA</sup>/Gr64f<sup>LEXA</sup>*

Figure S6:

- *w*<sup>1118</sup>
- +/+; *Gr64f-Gal4/UAS-GCaMP6f*; +/+
- +/+; *IR25a*<sup>1</sup>/+; +/+

- +/+; *IR25a<sup>1</sup>/IR25a<sup>2</sup>*; +/+
- +/+; +/+;  $\Delta$ *Gr64a-f*/+
- +/+; +/+;  $\Delta$ *Gr64a-f*/ $\Delta$ *Gr64a-f*

## METHOD DETAILS

### Tastants

The following tastants were used: DL-lactic acid, sucrose, NaCl, caffeine, acetic acid, propionic acid, hydrochloric acid (Sigma-Aldrich). Tastants were kept as 1 M stocks and diluted as necessary for experiments. The pH of tastants were adjusted where indicated using concentrated HCl or NaOH.

### Behavioral assays

Olfactory trap assays were designed to resemble previous protocols.<sup>65,66</sup> Groups of 40 flies were starved on 1% agar for 2 hours prior to the assay. Flies were lightly anesthetized with CO<sub>2</sub> and placed in the trap assay which consisted of a glass container (11 cm diameter x 11 cm height) containing two 25 mL glass flasks with 10 mL of either ddH<sub>2</sub>O or 250 mM lactic acid. The flasks were sealed with parafilm except for a small hole in the middle where a 1000 mL pipette tip was placed, stopping ~2 cm from the top of the solutions. The top of the tip was cut to ~8 mm and bottom of the tip was cut to ~2.5 mm, and the parafilm made contact with the pipette tip so that there were no potential exits from the flasks. The lid of the glass container had mesh holes larger than the flies, so parafilm was used to cover the mesh and 100 small holes poked uniformly throughout for airflow. Flies in the trap assay were placed at 29°C in the dark for ~18 hr. After, flies were anesthetized with CO<sub>2</sub> and the number of flies choosing the flask with water, lactic acid, or neither were counted and a preference index (PI) calculated as: ((# of flies in lactic acid flask)-(# of flies in water flask))/(total # of flies in either flask).

Binary choice feeding assays were performed similarly to previous descriptions.<sup>5</sup> Groups of 10 flies were starved on 1% agar for 1 day at 25°C prior to testing. For neural silencing with Kir2.1, expression was induced by placing flies at 29°C for three days prior to experiment to inactivate Gal80<sup>TS</sup> (2 days on food and 1 day on 1% agar). For all binary choice experiments, flies were transferred into vials containing six 10  $\mu$ L drops of alternating color. Each drop contained the specified concentration of tastant in 1% agar with either blue (0.125mg/mL Erioglaucine, FD and C Blue#1) or red (0.5mg/mL Amaranth, FD and C Red#2) dye. Color was balanced for each experiment (i.e., half of the replicates had lactic acid in red, water in blue, and half of the replicates had water in red, lactic acid in blue). Flies were allowed to feed for 2 hr at 29°C in the dark before freezing at -20°C. Abdomen color was scored under a dissection microscope as red, blue, purple, or no color. PI was calculated as ((# of flies labeled with tastant 1 color)-(# of flies labeled with tastant 2 color))/(total # of flies with color). Any vials with < 30% of flies feeding were excluded.

Capillary Feeder (CAFE) assays quantified over 24 hr were performed as previously described.<sup>67</sup> Briefly, 10 flies were starved for 5 hours and then placed in specialized 15 mL conical vials with access to two capillary tubes (A-M Systems 626000) containing water or two capillary tubes containing 250 mM lactic acid. All solutions contained 0.01% FD&C Blue No. 1 dye for visualization in photographs of the capillaries, which were taken once per hour for 24 hr with a Pentax Optio W90 handheld digital camera at 29°C. Two vials in each experiment did not contain flies and were used to control for the volume change due to evaporation. ImageJ was used to calculate the volume of solution consumed in each capillary from the photographs. PI was calculated by ((volume consumed of lactic acid)-(volume consumed of water))/(total volume consumed) for each 4-hr interval over 24 hr. An acute CAFE binary assay was used in other feeding experiments. For this assay, flies were starved 24 hr prior to the start and the same CAFE protocol was used except no dye was added to the solutions. The volume was marked by hand on the capillary tubes at the start and after 4 hr of feeding at 29°C. The distance between marks (i.e., volume consumed) was quantified in mm using a standard ruler under a dissection microscope. The mm was conferred to  $\mu$ L and the PI calculated as above. If vials consumed less than 0.5  $\mu$ L total volume they were excluded.

PER was performed as previously described.<sup>5,67</sup> For labellar PER, flies were mounted inside of 200  $\mu$ L pipette tips cut so that only the heads were exposed. Tubes were sealed with tape on the bottom and placed onto a slide with double sided tape. For tarsal PER, flies were immobilized on slides containing strips of myristic acid. For both assays, after a 1-2 hr recovery in a humidity chamber, flies were stimulated with water and allowed to drink until satiated (flies showing continued extension to water were excluded). Each fly was stimulated on either the labellum or tarsi with increasing concentrations of lactic acid followed by 500 mM sucrose as a positive control using a 20  $\mu$ L pipette attached to a 1 mL syringe. Each tastant was presented one time and water was offered in between each tastant to maintain satiation. For each tastant, flies showing clear extension were scored as 1 for that tastant, or 0 if not, and data are plotted as percent responding. Experiments were conducted over four different days, using 10-15 flies per genotype matched each day, and the order of genotypes stimulated each day was randomized.

For behavioral experiments with no olfactory organs, experimental flies were anesthetized with CO<sub>2</sub> after collection and sharp forceps used to remove the 3<sup>rd</sup> segment of the antennae and the maxillary palps of each fly. Control flies were anesthetized with CO<sub>2</sub> for the same duration. Both groups were allowed to recover for ~2 hr before being moved to starvation vials prior to the start of the experiments.

### Calcium imaging

*In vivo* GCaMP imaging of GRN axon terminals was performed as previously described.<sup>5</sup> Mated female flies aged 2-6 days were briefly anesthetized with CO<sub>2</sub> and placed in a custom chamber. Nail polish was used to secure the back of the neck and a small

amount of wax was applied to both sides of the proboscis in an extended position, covering the maxillary palps without touching the labellar sensilla. After 1 hr recovery in a humidity chamber, antennae were removed along with a small window of cuticle to expose the SEZ. Adult hemolymph-like (AHL) solution (108 mM NaCl, 5 mM KCl, 4 mM NaHCO<sub>3</sub>, 1 mM NaH<sub>2</sub>PO<sub>4</sub>, 5 mM HEPES, 15 mM ribose, 2mM Ca<sup>2+</sup>, 8.2mM Mg<sup>2+</sup>, pH 7.5) was immediately applied. Air sacs and fat were removed and the esophagus was clipped and removed for clear visualization of the SEZ.

A Leica SP5 II Confocal microscope was used to capture GCaMP6f fluorescence with a 25x water immersion objective. The SEZ was imaged at a zoom of 4x, line speed of 8000 Hz, line accumulation of 2, and resolution of 512 × 512 pixels. Pinhole was opened to 2.86 AU. For each taste stimulation, 15 total seconds were recorded. For 1 s stimulations, this consisted of 5 s baseline, 1 s stimulation, 9 s post-stimulation. For 4 s stimulations, this consisted of 5 s baseline, 4 s stimulation, 6 s post-stimulation. A pulled capillary filed down to fit over both labellar palps was filled with tastant and positioned close to the labellum with a micromanipulator. For the stimulation, the micromanipulator was manually moved over the labellum and then removed from the labellum after 1 or 4 s. The stimulator was washed with water in between tastants of differing solutions.

The maximum change in fluorescence (peak  $\Delta F/F_0$  or  $\Delta F_1/F_0$ ) for “onset” peaks was calculated using peak intensity (average of 3 time points) minus the average baseline intensity (10 time points), divided by the baseline. For “removal” peaks with 4 s stimulation, peak  $\Delta F_2/F_0$  was calculated using peak intensity during stimulus removal (average of 3 time points) minus the minimum intensity prior to removal (3 time points), divided by baseline fluorescence. ImageJ was used to quantify fluorescence changes and create heat-maps. In the calcium imaging experiments using *Gr64a-f* mutants, ~15% showed a significant response to water (with stimulus onset or removal) and were removed from the final dataset.

### Survival assay

Adult, mated female flies, were collected and placed on the indicated solution as the only food option in 1% agar at room temperature at 3 days old. Flies were flipped onto fresh solution in agar every two days. A total of ten flies were in each vial and the number dead and alive counted once per day, and plotted as the % of flies alive. All solutions were run in parallel.

### Immunohistochemistry

Brain immunofluorescence was performed as previously described.<sup>5</sup> Primary antibodies used were rabbit anti-GFP (1:1000, Invitrogen) and mouse anti-brp (1:50, DSHB #nc82). Secondary antibodies used were goat anti-rabbit Alexa 488 and goat anti-mouse Alexa 546 (1:200, Invitrogen). Images were acquired using a Leica SP5 II Confocal microscope under 25x objective. Images were processed in ImageJ.

### QUANTIFICATION AND STATISTICAL ANALYSIS

Statistical tests were performed using GraphPad Prism 6 software and are stated in the figure legends along with the sample sizes and what is considered a biological replicate for each experiment. Sample sizes were generally determined *a priori* based on the variance and effect sizes seen in similar previous experiments. Experimental conditions and genotype controls were always run in parallel. In the rare occurrence that a data point appeared to be a visible outlier, a Grubb's test was performed and excluded from the dataset if meeting a significance value of  $< 0.05$ . Significant differences are denoted as \* $p < 0.05$ , \*\* $p < 0.01$ , \*\*\* $p < 0.001$ .